Langmuir

Subscriber access provided by Northwestern Univ. Library

Article

Responsive Wormlike Micelles from Dynamic Covalent Surfactants

Jan H. van Esch, Rienk Eelkema, Ger J. M. Koper, Job Boekhoven, Christophe B. Minkenberg, Ben Norder, and Bart Homan

Langmuir, **Just Accepted Manuscript** • DOI: 10.1021/la302294r • Publication Date (Web): 08 Aug 2012

Downloaded from http://pubs.acs.org on September 7, 2012

Just Accepted

"Just Accepted" manuscripts have been peer-reviewed and accepted for publication. They are posted online prior to technical editing, formatting for publication and author proofing. The American Chemical Society provides "Just Accepted" as a free service to the research community to expedite the dissemination of scientific material as soon as possible after acceptance. "Just Accepted" manuscripts appear in full in PDF format accompanied by an HTML abstract. "Just Accepted" manuscripts have been fully peer reviewed, but should not be considered the official version of record. They are accessible to all readers and citable by the Digital Object Identifier (DOI®). "Just Accepted" is an optional service offered to authors. Therefore, the "Just Accepted" Web site may not include all articles that will be published in the journal. After a manuscript is technically edited and formatted, it will be removed from the "Just Accepted" Web site and published as an ASAP article. Note that technical editing may introduce minor changes to the manuscript text and/or graphics which could affect content, and all legal disclaimers and ethical guidelines that apply to the journal pertain. ACS cannot be held responsible for errors or consequences arising from the use of information contained in these "Just Accepted" manuscripts.

ACS Publications
High quality. High impact.

Langmuir is published by the American Chemical Society. 1155 Sixteenth Street N.W., Washington, DC 20036

Published by American Chemical Society. Copyright © American Chemical Society. However, no copyright claim is made to original U.S. Government works, or works produced by employees of any Commonwealth realm Crown government in the course of their duties.

Responsive Wormlike Micelles from Dynamic Covalent Surfactants

*Christophe B. Minkenberg, Bart Homan, Job Boekhoven, Ben Norder, Ger J. M. Koper, Rienk Eelkema and Jan H. van Esch**

Self-Assembling Systems, Department of Chemical Engineering, Delft University of Technology, Julianalaan 136, 2628 BL Delft, The Netherlands.

j.h.vanesch@tudelft.nl

RECEIVED DATE (to be automatically inserted after your manuscript is accepted if required according to the journal that you are submitting your paper to)

ABSTRACT Dynamic covalent chemistry is a powerful tool for the construction of adaptive and stimuli responsive nanosystems. Here we report on the spontaneous formation of dynamic covalent wormlike micelles from imine-based gemini surfactants, formed upon mixing aqueous solutions of two complementary non-surface active precursors. Resulting from the reversibility of the dynamic covalent imine bond, the wormlike micelles can be switched between an isotropic solution and the assembled state, triggered by pH and temperature. Thermodynamic modeling of the reaction equilibria shows that, although mixtures of single and double tailed surfactants are formed, it is mainly the double tailed surfactant that assembles into the wormlike micelles.

KEYWORDS Dynamic covalent chemistry, imine, gemini surfactant, responsive surfactant, wormlike micelle

Introduction

Surfactant self-assembly is of particular interest for medical and biological applications and in numerous industrial and domestic processes. A specific class of surfactants, gemini surfactants, have shown great potential for gene transfection[1] and are used in cosmetics and as polymer substitutes because of their visco-elastic properties.[2,3] These diverse material properties are directly linked to the morphology of the gemini surfactant assemblies, which can vary from, amongst others, spherical to disk-like and worm-like micelles as well as vesicles.[4-8] Gemini surfactant aggregate morphology has successfully been controlled by molecular design[9-13], variation of counter ions[9-13] and with co-surfactants[14-16], and by external stimuli like pH[17-20] and temperature[5,12]. Despite their potential applications, so far wormlike micellar systems that can be switched reversibly between assembly and homogeneous aqueous solution have not been reported. Dynamic covalent chemistry has proven to be a powerful tool for the construction of adaptive and reversible systems[21-29] and already led to a variety of supramolecular assemblies like gels[30-32] and nanorods[33,34]. Recently, we and others successfully exploited dynamic covalent surfactant chemistry for the formation of responsive micelles and vesicles.[35-40] Also the autocatalytic formation of micelles, vesicles and wormlike micelles has been demonstrated, however, always starting from heterogeneous mixtures of insoluble precursors.[37]

Here we report on dynamic covalent gemini surfactants that, upon formation, assemble into wormlike micelles. This switchable surfactant system is formed in situ and at ambient conditions through the formation of a dynamic covalent bond between non-amphiphilic, water-soluble precursors. Triggered by pH or temperature, these systems can be switched reversibly between an assembled state of the intact surfactants and isotropic solution of non-assembled precursor compounds. In this paper we introduce six different dynamic covalent gemini-surfactants that form wormlike micellar assemblies.

Materials and Methods

Starting materials and amines $\mathbf{T_5}$, $\mathbf{T_7}$ and $\mathbf{T_8}$ (1-pentylamine, 1-heptylamine, and 1-octylamine, respectively) were obtained from Sigma Aldrich and Acros Organics and were used without further

purification. ^{1}H-NMR and ^{13}C-NMR spectra for structure determination were recorded at room temperature on a Bruker Avance-400 spectrometer (at 400 MHz for ^{1}H) and a Varian Inova-300 spectrometer (at 75 MHz for ^{13}C). Chemical shift values are denoted in δ values (ppm) relative to residual solvent peaks ($CDCl_3$, ^{1}H δ = 7.26; D_2O, ^{1}H δ = 4.79; ^{13}C-NMR in D_2O was referenced to internal dioxane (δ = 67.19)). The splitting patterns are noted as follows: s (singlet), d (doublet), t (triplet), q (quartet), m (multiplet). LC-MS was performed a Shimadzu LCMS-2010A instrument using a Xbridge shield RP 18 5µm 46*150 mm column using a H_2O/ethanol gradient acidified with 0.1% TFA with an injection volume of 20µl and a flow of 1.0 ml/min. Imine formation was studied by ^{1}H-NMR on a Varian Inova-300 spectrometer (at 300 MHz for ^{1}H), using a water presaturation sequence in a 9:1 vol.% H_2O/D_2O mixture.

General synthetic procedure for aldehyde headgroups H_3 and H_6. 1.5 g (7 mmol) p-(bromopropyl)benzaldehyde was dissolved in 15 ml dry acetone. After this 0.4 g (3.3 mmol) tetramethyl-propanediamine (for **H_3**) or 0.6 g (3.3 mmol) tetramethyl-hexanediamine (for **H_6**) was added and the mixture was refluxed overnight. Next, the mixture was cooled to room temperature and subsequently to 0°C on an ice bath, resulting in precipitation of the crude product. The reaction mixture was filtered, followed by washing the residue with dry acetone. Finally, the residue was dried under vacuum, yielding the pure product as yellow powder in typical yields of 80 to 90%. Headgroup **H_3** ^{1}H-NMR (D_2O): 9.89 (s, 2H), 7.88 (d, 4H, J = 8.0 Hz), 7.47 (d, 4H, J = 7.9 Hz), 3.33 (m, 8H), 3.06 (s, 12H), 2.81 (t, 4H, J = 7.0 Hz), 2.13 (m, 6H). ^{13}C-NMR (D_2O): 196.6, 148.9, 134.8, 131.2, 129.9, 64.24, 60.3, 51.6, 32.2, 23.4, 17.3. HPLC retention time: 6.34 min; λ_{max} (EtOH / H_2O, 0.1% TFA) 221 nm, elutes with 23% EtOH. MS (ESI+) m/z calculated for $C_{29}H_{40}F_3N_2O_4^+$ $(M+TFA)^+$: 537.3. Found: 537.4. Headgroup **H_6** ^{1}H-NMR (D_2O): 9.80 (s, 2H), 7.81 (d, 4H, J = 7.9 Hz), 7.45 (d, 4H, J = 7.9 Hz), 3.22 (m, 8H), 2.99 (s, 12H), 2.77 (t, 4H, J = 7.1 Hz), 2.08 (m, 4H), 1.50 (s, 4H) 1.21 (s, 4H). ^{13}C-NMR (D_2O): 196.6, 149.2, 134.8, 131.2, 130.1, 63.94, 63.1, 51.5, 32.2, 25.7, 23.9, 22.3. HPLC retention time: 10.08 min; λ_{max} (EtOH / H_2O, 0.1% TFA) 221 nm, elutes with 32% EtOH. MS (ESI+) m/z calculated for $C_{32}H_{46}F_3N_2O_4^+$ $(M+TFA)^+$: 579.3. Found: 579.3.

Preparation of the Gemini surfactant solutions

Method A: An aqueous solution containing the aldehyde headgroup (**H_3** or **H_6**) and amine in a 1:2 molar ratio was obtained by mixing the desired amounts of aqueous solution of the headgroup with an aqueous solution containing typically 10-20 mM of the amine. Method A was applied if the solubility of the amine (e.g. 25 mM for heptyl amine at 20°C [41]) allowed dissolution of required amount of amine.

Method B: An aqueous solution containing the aldehyde headgroup (**H_3** or **H_6**) and amine in a 1:2 molar ratio was obtained by adding the desired amounts of an aqueous solution of the headgroup to a weighted amount of the neat amine, followed by vortexing during 1-3 minutes. Method B was applied if the solubility of the amine (e.g. 25 mM for heptyl amine at 20°C [41]) prevented the preparation of sufficiently concentrated aqueous solutions of the amine.

Surface tension measurements for CAC determination. Surfactant critical aggregation concentrations (CACs) were determined by surface tension measurements on a KRÜSS FM40 Easy Drop, using a syringe pump and a CCD camera, at ambient temperature. The CACs were determined by first preparing a stock solution containing the aldehyde and amine in 1:2 molar ratio by Method A (see above). From this stock solution a dilution series of bisaldehyde **H_3** or **H_6** with amines **T_5**, **T_7** and **T_8** in a 1:2 (head:tail) ratio in MilliQ water was prepared (equilibrated at 25°C and pH = 10.5 due to added amine). By plotting the surface tension vs concentration, with the concentration plotted on a logarithmic scale, the CAC is determined at the intercept of the two crossing lines where the decreasing surface tension becomes constant (see Figure S2 in the Supporting Information).

Nile Red fluorescence measurements. Fluorescence spectroscopy was performed on a Jasco J-815 CD-spectrometer equipped with emission accessory. The temperature was controlled using a Jasco PFD 4252/15 Peltier temperature unit. All samples contained Nile Red probe in 2 μM concentrations and were excited at 550 nm. The maximum Nile Red emission wavelength (λ_{max}) was determined at building block concentrations of $[\mathbf{H}_x]_0$ = 100 mM and $[\mathbf{T}_y]_0$ = 200 mM (equilibrated at 25°C, pH = 10.5 due to the added amine).

Dynamic Light Scattering (DLS). Dynamic Light Scattering was performed in MilliQ water at 25°C on a ZetaSizer Nano series Nano-ZS (Malvern Instruments). The samples were prepared by Method B at concentrations of $[\mathbf{H}_x]_0$ = 100 mM and $[\mathbf{T}_y]_0$ = 200 mM (equilibrated at 25°C, pH = 10.5 due to the added amine). The autocorrelation functions were fitted with the Multiple Narrow Modes Algorithm for bimodal distributions, as implemented in the Zetasizer software.

Cryo TEM. Pictures were obtained on a Philips CM10 electron microscope operating at 100 kV. Samples were prepared by depositing 2.5µl of aqueous mixture on a carbon coated grid full of holes (Quantifoil 3.5/1, Quantifoil micro tools GmbH, Jena, Germany). After blotting away the excess liquid, the grids were plunged quickly in liquid ethane. Blotting was performed at 100% relative humidity to prevent evaporation of water. Frozen-hydrated specimens were mounted in a cryo-holder (Gatan, model 626). Micrographs were recorded under low-dose conditions on a slow-scan CCD camera (Gatan, model 794).

pH-Controlled aggregate dissociation. Solutions were prepared by Method B at 50 mM concentrations (50 mM [$\mathbf{H_3}$], 100 mM [$\mathbf{T_7}$]) and equilibrated at 25°C and pH 10.3 in MilliQ water. After this, the pH of the solution was adjusted to the desired pH by addition of aqueous HBr. Nile Red was added to each sample in probe concentrations of 1 µM and excited at 550 nm. The emission of the Nile Red probe itself was not affected by salt concentration (see Figure S6 in the Supporting Information) or pH[35,42].

Temperature-controlled aggregate dissociation. An $\mathbf{H_3}\bullet\mathbf{T_7}$ solution was prepared by Method A at a concentration of 8mM [$\mathbf{H_3}$] and 16mM [$\mathbf{T_7}$] in MilliQ water at 20°C. The pH of the solution was ~10.3 due to the added amine. Nile Red was added to the sample in probe concentrations of 1 µM and excited at 550 nm. The sample was subsequently heated from 20°C to 70°C in steps of 10°C with equilibration times between heating steps of 15 minutes. After each 15 minutes the Nile Red emission was measured. The emission of the Nile Red probe itself was not affected within this temperature region (see Figure S6 in the Supporting Information).

Rheology. Measurements were performed on a TA Instruments AR-G2 rheometer using a parallel plate geometry with 40 mm diameter, between which a sample of 100 mM surfactant solution prepared by Method B was placed. All measurements were performed in the lineair visco-elastic region.

Results

We developed six different dynamic covalent gemini-surfactants by mixing a bisaldehyde functionalized quaternary ammonium headgroup ($\mathbf{H_3}$ or $\mathbf{H_6}$) with a primary amine functionalized tail (1-pentylamine $\mathbf{T_5}$, 1-heptylamine $\mathbf{T_7}$, or 1-octylamine $\mathbf{T_8}$) in water (Scheme 1). The spacer length between the two headgroups of building blocks $\mathbf{H_3}$ and $\mathbf{H_6}$ is fixed at either 3 or 6 methylene units, while the apolar tails are covalently connected to the headgroup by reversible imine bonds, resulting in surfactant systems $\mathbf{H_3{\bullet}T_5}$, $\mathbf{H_3{\bullet}T_7}$, $\mathbf{H_3{\bullet}T_8}$, $\mathbf{H_6{\bullet}T_5}$, $\mathbf{H_6{\bullet}T_7}$ and $\mathbf{H_6{\bullet}T_8}$ (Scheme 1, e.g. $\mathbf{H_3{\bullet}T_5}$ indicates an unspecified surfactant mixture resulting from reaction of $\mathbf{H_3}$ and $\mathbf{T_5}$), The surfactant systems consist of a mixture of both mono- and disubstituted surfactants, as well as remaining unreacted starting materials, with the ratios between all constituents depending on the conversion.

Scheme 1. Dynamic formation and assembly of dynamic covalent gemini surfactants, forming single tailed $\mathbf{H_x(T_y)_1}$ and double tailed $\mathbf{H_x(T_y)_2}$ compounds.

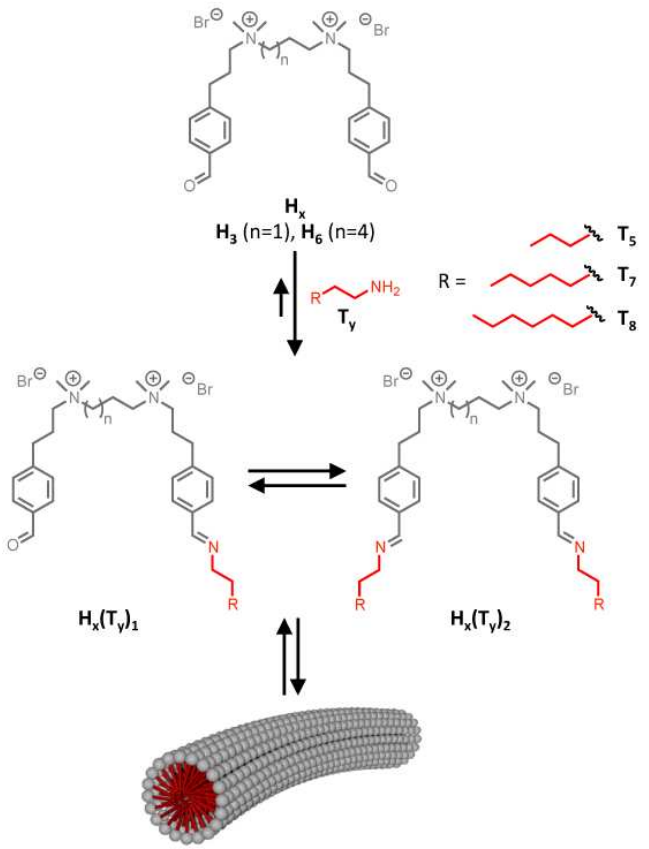

The gemini surfactants were prepared from non-surface active aqueous aldehyde and amine stock solutions and mixed in a 1:2 molar ratio to achieve a 1:1 aldehyde:amine functional group ratio, at ambient conditions (Method A, see Experimental). Within a minute after mixing, foaming, but otherwise transparent and non-viscous solutions were obtained. Alternatively, solutions of the gemini surfactants at concentrations exceeding the solubility of the amines (typically 25 mM for heptyl amine at 20°C [41]) were obtained by vortexing a concentrated solution of the ammonium aldehyde with the required amount of neat amine (Method B, see Experimental). Within minutes, the amine was completely dissolved and transparent solutions were obtained. Critical aggregation concentrations were determined by surface tension measurements (Table 1 and Figure S2 in the Supporting Information) and are typically in the millimolar range. Without the addition of hydrophobic tails $\mathbf{T_y}$ the cationic headgroups $\mathbf{H_3}$ and $\mathbf{H_6}$ are found to modify the surface tension only slightly, and monotonously, in stark contrast to the drastic changes in surface tension caused by the dynamic surfactants near the CAC (see the supporting information). Surface tension data showed that the CACs significantly decrease with increasing tail length **T**, while the spacer length of **H** has only a small effect on the CAC. The same

surface tension data have been analyzed using the Gibbs adsorption isotherm to extract information on the specific surface area (σ) of the surfactant molecules (Table 1). The thus obtained values are for the single tailed surfactants that are dominant below the CAC, see Figure 2. The T_5-surfactants appear to have a larger specific surface area than their longer tailed equivalents, which is probably due to the higher solubility of the shorter tails. The spacer length does not have a strong effect on the specific surface area. Fluorescence spectroscopy on dynamic covalent gemini surfactant solutions ($[\mathbf{H}_x]_0$ = 100 mM and $[\mathbf{T}_y]_0$ = 200 mM), doped with solvatochromic probe Nile Red[42,43], showed emission maxima of 640±2 nm for all investigated systems, which indicates that all formed assemblies have a similar hydrophobicity, in-between micelles and vesicles made of similar components.[35,36,42,43]

Table 1. Critical aggregation concentrations, specific surface area, and aggregate sizes.

Surfactant System	CAC [a] (mM $[\mathbf{H}]_0$)	σ [a] (nm^2)	D_h [b] (nm)		L_{ee} [c] (nm)
H_3●T_5	10 ± 1	2.2 ± 0.3	2.6 ± 1	4.4 ± 1	
H_6●T_5	12.5 ± 1	2.2 ± 0.3	3.3 ± 1		
H_3●T_7	2 ± 1	1.0 ± 0.2	2.5 ± 1	14.4 ± 1	30 ± 10
H_6●T_7	3 ± 1	0.92 ± 0.2	2.0 ± 1	8.4 ± 1	
H_3●T_8	1.5 ± 1	0.96 ± 0.2	2.2 ± 1	18.0 ± 1	24 ± 7
H_6●T_8	1.5 ± 1	0.80 ± 0.2	2.0 ± 1	8.6 ± 1	13 ± 7

[a] measured by surface tension; [b] according to Multiple Narrow Modes Algorithm;
[c] determined from cryo-TEM pictures.

The sizes of the formed assemblies were determined by dynamic light scattering (DLS). DLS was performed at concentrations of $[\mathbf{H_x}]_0$ = 100 mM and $[\mathbf{T_y}]_0$ = 200 mM, which is well above the CAC of all systems. We observed that the measured autocorrelation functions showed a second plateau region at roughly $\tau = 10^2$ μs, which is indicative for a second aggregate population or dimension (see Figure S3 in the Supporting Information). Therefore, the obtained autocorrelation functions were fit with a Multiple

Narrow Modes Algorithm, with the assumption that there is a bimodal size distribution. With the exception of $\mathbf{H_6{\bullet}T_5}$, two hydrodynamic diameters (D_h) were found for each surfactant system (Table 1). The smaller diameters were around $1 \leq D_h \leq 4$ nm and the larger diameters were around $4 \leq D_h \leq 19$ nm, which suggests the presence of spherical micelles coexisting with larger aggregates.[44]

The morphologies of the assemblies of $\mathbf{H_3{\bullet}T_5}$, $\mathbf{H_3{\bullet}T_7}$, $\mathbf{H_6{\bullet}T_7}$, $\mathbf{H_3{\bullet}T_8}$ and $\mathbf{H_6{\bullet}T_8}$ were investigated in more detail by cryo-TEM. At concentrations of $[\mathbf{H_x}]_0$ = 100 mM and $[\mathbf{T_y}]_0$ = 200 mM small, isolated wormlike micelles were visible for $\mathbf{H_3{\bullet}T_5}$ (Figure 1a), whereas in the case of $\mathbf{H_3{\bullet}T_7}$ (Figure 1b), $\mathbf{H_3{\bullet}T_8}$ and $\mathbf{H_6{\bullet}T_8}$ (see Figure S4 in the Supporting Information) loosely connected wormlike micelles were observed. The end-to-end distances (L_{ee}) determined with cryo-TEM for the wormlike systems are 30 ± 10 nm for $\mathbf{H_3{\bullet}T_7}$, 24 ± 7 nm for $\mathbf{H_3{\bullet}T_8}$ and 13 ± 7 nm for $\mathbf{H_6{\bullet}T_8}$, which is in good agreement with the size of the larger aggregates observed by DLS (Table 1). Although there is only a moderate influence of the molecular structure on the morphology, the micellar length is significantly longer for the $\mathbf{H_3}$-based surfactants, and also seems to increase with increasing tail length. These results suggest that the aspect ratio of the worm-like micelles increases with increasing anisotropy of the surfactant, which is in line with earlier observations for conventional cationic gemini surfactants.[6] Within a simple model of wormlike micelles the length of the micelles is controlled by the balance between the entropy associated with the size distribution and the so called end cap energy associated with the termination of the worm-like micelles.[45] The longer tail surfactant molecules are more stretched to form an end cap which results in a higher end cap energy and hence longer micellar lengths. The micellar length of the dynamic covalent surfactants reported here seems to be consistently smaller than for comparable conventional gemini surfactants, suggesting that wormlike micelles from our dynamic covalent gemini surfactants have lower end cap energies, compared to conventional wormlike micellar systems.[45-48]

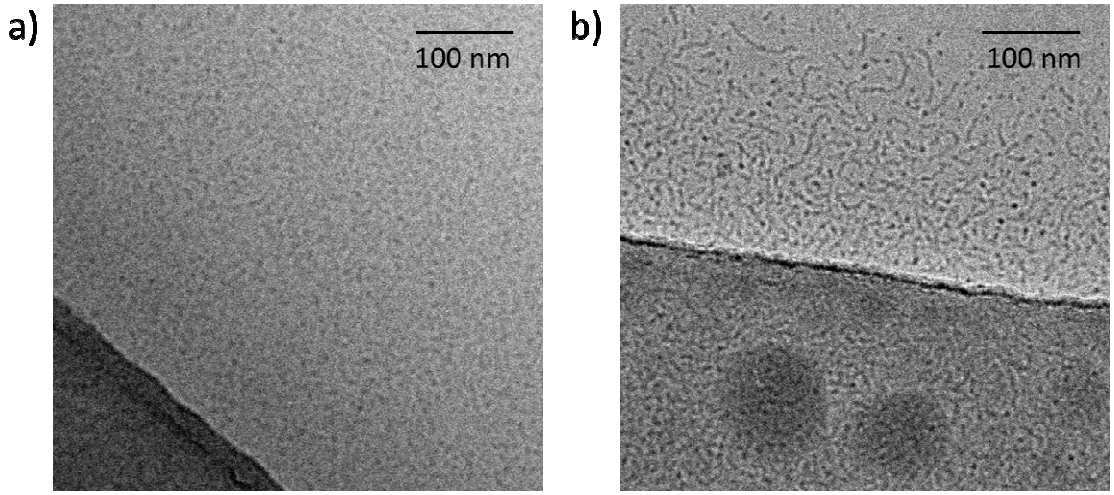

Figure 1. Cryo-TEM micrographs of a) $\mathbf{H_3 \bullet T_5}$ and b) $\mathbf{H_3 \bullet T_7}$ showing wormlike micelles. The concentrations of the surfactant solutions are $[\mathbf{H_x}]_0$ = 100mM and $[\mathbf{T_y}]$ = 200mM, equilibrated at room temperature and pH 10.5.

Judging from the appearance of surfactant aggregates, imine surfactants must have formed above the CACs, but it remains unclear whether the observed morphologies are formed from single or double tail imine surfactants, or their mixtures. To investigate the surfactant composition, imine formation was studied by ^{1}H-NMR for different concentrations of bisaldehyde $\mathbf{H_3}$ with amines $\mathbf{T_5}$ and $\mathbf{T_7}$, at constant 1:2 molar ratio. NMR showed the formation of imines already at millimolar concentrations (Figure 2a and b). The observation of separate peaks for the aldehyde $\mathbf{H_3}$ CH=O signals, the mono-imine $\mathbf{H_3(T_y)_1}$ CH=O and CH=N signals and the bisimine $\mathbf{H_3(T_y)_2}$ CH=N signals indicates that the imine formation equilibrium is slow on the NMR timescale. It should be noted that the bis-imine CH=N signals can be easily distinguished from the mono-imine CH=N signals, because of the non-symmetrical multiplicity of the aromatic protons of mono-imine $\mathbf{H_3(T_y)_1}$.

At higher concentrations the mono- and bisimine peaks gradually shift upfield (Figure 2 c and d), whereas the $\mathbf{H_3}$ CH=O chemical shift remains the same, indicating self-assembly of the mono- and bis-imine surfactant molecules, but not of the $\mathbf{H_3}$ headgroups.[35,36] This concentration dependent chemical shift indicates that association into micellar structures involves an equilibrium that is fast on the NMR

time scale. The association-induced upfield shift is larger for the bis-imines than for the mono-imines, which indicates that there is a preference of double tailed surfactants to be incorporated in **H_3●T_5** and **H_3●T_7** micelles. Unfortunately, the NMR signals for the amines were not sufficiently resolved to draw conclusions on their chemical environment, and therefore we cannot exclude their possible incorporation into micelles. It should be noted, however, that the concentration of unreacted amine in solution is very low, as most of the amine is converted to the imine. Moreover, both **H_3●T_5** and **H_3●T_7** imine formation curves show a large increase in double tailed surfactant formation at concentrations above the CAC (Figure 2), which is indicative for aggregation-induced stabilization of the imine bond, leading to the enhanced formation of double tailed surfactants.[35]

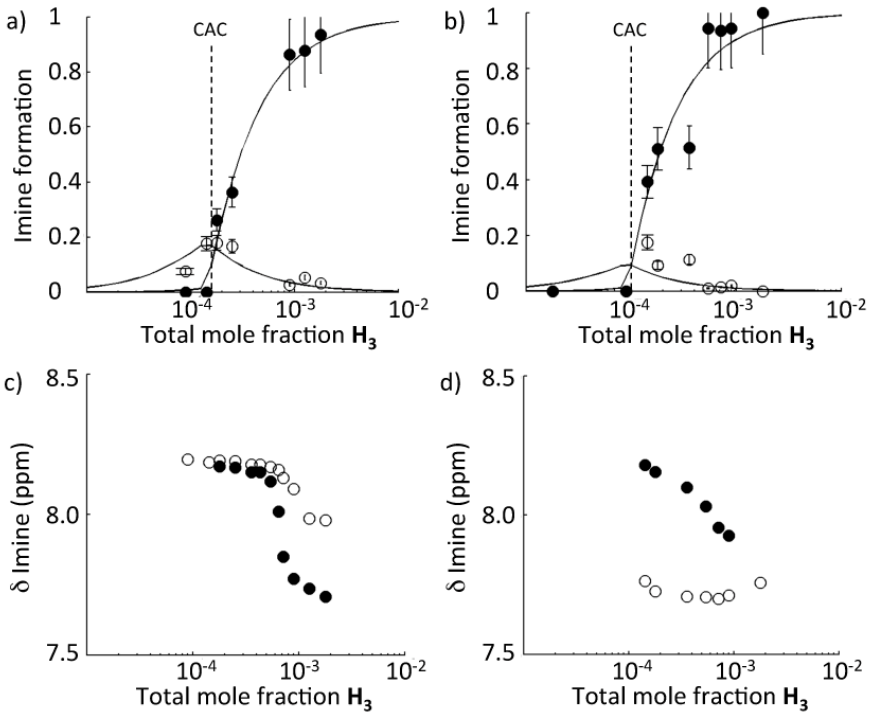

Figure 2. Imine formation curves (a,b) and concentration dependent imine CH=N chemical shifts (c,d) as determined for **H_3●T_5** (a,c) and **H_3●T_7** (b,d) by ^{1}H-NMR at 25°C. For all graphs: mono-imine $\mathbf{H_x(T_y)_1}$ surfactants (open spheres), bisimine $\mathbf{H_x(T_y)_2}$ surfactants (closed spheres), plotted against the mole fraction of initially added **H_3**. The solid lines are fits of a thermodynamic model for imine formation (vide infra) to the experimental data points.

Because most species involved in the imine formation equilibrium could be observed by ^{1}H NMR, the present system allows for a quantitative analysis of the imine formation and aggregation equilibria (Figure 2). Since all surfactant solutions were analyzed at equilibrium conditions, we expect that the single tailed ($\mathbf{H_x(T_y)_1}$) and double tailed surfactants ($\mathbf{H_x(T_y)_2}$) and their assemblies, $\mathbf{M_y}$ and $\mathbf{M_{yy}}$ respectively, are formed under thermodynamic control. Hence, it should be possible to quantitatively describe imine formation and aggregation by a thermodynamic model, entirely based on imine formation and surfactant aggregation equilibria (see Supporting Information). In this model formation of surfactants $\mathbf{H_x(T_y)_1}$ and $\mathbf{H_x(T_y)_2}$ and assemblies $\mathbf{M_y}$ and $\mathbf{M_{yy}}$ were described as coupled equilibria with imine formation constants K_y and K_{yy} and aggregation constants $K_{m,y}$ and $K_{m,yy}$ respectively (Scheme 2). The number of $\mathbf{H_x(T_y)_1}$ and $\mathbf{H_x(T_y)_2}$ surfactants in assemblies $\mathbf{M_y}$ and $\mathbf{M_{yy}}$ is limited by their aggregation numbers N_y and $N_{yy,}$ respectively, which are assumed to be constant within the experimental concentration range.

Scheme 2. Imine formation and surfactant aggregation equilibria

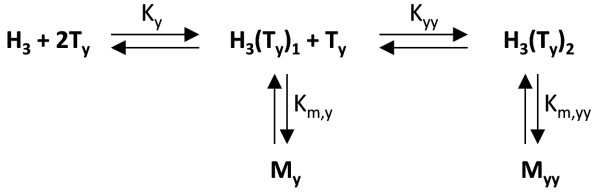

The model described above provided a good fit to the imine formation data (see Figure 2), with dimensionless imine formation constants of $pK_5 = 3.3 \pm 0.2$ ($\mathbf{H_3(T_5)_1}$) and $pK_7 = 3.2 \pm 0.2$ ($\mathbf{H_3(T_7)_1}$) for the single tailed surfactants. For double tailed surfactants $\mathbf{H_3(T_5)_2}$ and $\mathbf{H_3(T_7)_2}$, imine formation constants of $pK_{55} = pK_{77} = 2.5 \pm 0.2$ were found. The values are slightly smaller than pK_5 and pK_7, which might be indicative for a small anti-cooperative effect for binding of the second hydrophobic tail to the single tailed surfactant (Table 2). The aggregation constants were determined at $pK_{m,5} = 3.5 \pm 0.2$ ($\mathbf{H_3(T_5)_1}$) and $pK_{m,7} = 4.0 \pm 0.2$ ($\mathbf{H_3(T_7)_1}$) for the single tailed surfactants. The more hydrophobic double tailed $\mathbf{H_3(T_5)_2}$ and $\mathbf{H_3(T_7)_2}$ surfactants exhibit aggregation constants of $pK_{m,55} = 5.2 \pm 0.2$ and $pK_{m,77} = 5.7 \pm 0.2$ (Table 2). These latter values are significantly larger than the single tailed surfactant

aggregation constants $pK_{m,5}$ and $pK_{m,7}$, which reflects the increase in hydrophobicity in the double tail surfactants as compared to their single tail analogues.

Table 2. Imine formation equilibrium constants, aggregation constants and calculated CAC values for surfactant systems **H_3●T_5** and **H_3●T_7** in water.

Surfactant system	pK_y [a]	pK_{yy} [a]	$pK_{m,y}$ [a]	$pK_{m,yy}$ [a]	CAC_y (mM $[\mathbf{H}]_0$) [b]	CAC_{yy} (mM $[\mathbf{H}]_0$) [b]
H_3●T_5	3.3 ± 0.2	2.5 ± 0.2	3.5 ± 0.2	5.2 ± 0.2	> 100	9 ± 2
H_3●T_7	3.2 ± 0.2	2.5 ± 0.2	4.0 ± 0.2	5.7 ± 0.2	> 100	5 ± 2

[a] Dimensionless values; [b] these CAC values are calculated from $pK_{m,yy}$, see the supporting information.

It should be noted that these imine association and aggregation constants are dimensionless and can be converted to constants with a mM^{-1} dimension after correction for the water concentration in water (55.6 M^{-1}). The CACs are inversely related to the surfactant aggregation constants $pK_{m,y}$ and $pK_{m,yy}$ and amount to 20 ± 8 mM **H_3(T_5)$_1$** and 0.4 ± 0.2 mM **H_3(T_5)$_2$** for surfactant system **H_3●T_5**. For **H_3●T_7**, CACs of 6 ± 3 mM **H_3(T_7)$_1$** and (12 ± 5)*10^{-2} mM **H_3(T_7)$_2$** were calculated. However, these CACs are expressed in single tailed and double tailed surfactant concentrations, whereas the experimental CACs in Table 1 have been given in initial aldehyde concentrations $[\mathbf{H}]_0$. Therefore the calculated CACs for double and single tailed surfactant formation are expressed in $[\mathbf{H}]_0$ concentrations, which makes it possible to directly compare the calculated CACs with the experimental CACs. The calculated CACs for both **H_3(T_5)$_1$** and **H_3(T_7)$_1$** single tailed surfactants are above 100 mM $[\mathbf{H}]_0$, which indicates that the single tailed surfactants do not aggregate under the experimental conditions. From the data in Table 2 CACs for double tailed surfactants are calculated to be 9 ± 2 mM mM $[\mathbf{H}]_0$ for **H_3(T_5)$_2$** and 5 ± 2 mM $[\mathbf{H}]_0$ for **H_3(T_7)$_2$** (Table 2), which are in good agreement with the experimental CACs in Table 1, considering experimental errors and assumptions made. Above these calculated CACs (Table 2), the molar fraction of double tailed surfactant increases at the expense of single tailed surfactant (Figure 2a

and 2b). These results clearly indicate that both $\mathbf{H_3{\bullet}T_5}$ and $\mathbf{H_3{\bullet}T_7}$ aggregates are formed by self assembly of mainly the double tailed surfactants with possibly minor fractions of the single tail surfactants and free amines, which is also corroborated by the concentration-dependent changes in the chemical shifts of single and double tailed surfactants (Figure 2c). It can be concluded from these results that imine formation and aggregation of single and double tailed surfactants for dynamic covalent $\mathbf{H_3{\bullet}T_5}$ micelles and $\mathbf{H_3{\bullet}T_7}$ wormlike micelles can be described with a simple thermodynamic model, which suggests that both aggregation morphologies are equilibrium structures.

To investigate to what extent the formation of dynamic covalent wormlike aggregates affects the solution viscosity, rheological properties of the three wormlike micelle-forming systems were investigated. Dynamic viscosities were measured at angular frequencies between 0.1 and 100 rad/s within the linear visco-elastic region. Samples were prepared at $[\mathbf{H_x}]_0$ = 100 mM and $[\mathbf{T_y}]_0$ = 200 mM, which are the same concentrations as used for the cryo-TEM experiments. At these concentrations, the imine formation equilibrium is fully positioned towards double tailed surfactants (Figure 2). Dynamic viscosities from 1 to 60 mPa*s, with storage and loss moduli in the milli-Pascal range, were measured for all dynamic covalent wormlike micellar systems, which is of the same order of magnitude as pure water (see Figure S5 in the Supporting Information). The rheological properties of our dynamic covalent wormlike micelles strongly differ from comparable wormlike micelle forming covalently fixed surfactant systems, which are highly viscous solutions under the mentioned experimental conditions. From the rheological data in combination with the observed dimensions and end-to-end distances of the worms as observed by cryo-TEM, it can be concluded that the near Newtonian behavior of these dynamic covalent wormlike micelles can be attributed to the relative small length and large flexibility of the worms.

In contrast to conventional gemini surfactant systems, our wormlike micelle systems are formed by the formation of reversible covalent bonds between water-soluble precursors, which should make the system responsive to external stimuli. Since the position of the imine formation equilibrium can be

directed by pH and temperature, it should be possible to repeatedly switch self-assembly on and off by shifting the equilibrium towards the surfactant or its precursors and vice versa.[35,36] The pH-triggered demicellization of a wormlike micellar $\mathbf{H_3 \bullet T_7}$ solution was examined using fluorescence emission spectroscopy, with Nile Red as a hydrophobic probe. Titration with aqueous HBr of a $\mathbf{H_3 \bullet T_7}$ solution (50 mM [$\mathbf{H_3}$], 100 mM [$\mathbf{T_7}$]) equilibrated at pH 10.3) led, in less than a minute, to a red shift in the Nile Red emission from 640 nm to 658 nm, indicative of the departure of Nile Red from the hydrophobic interior of the assembly (Figure 3a). At pH 3.9 an emission maximum of 658 nm was observed, corresponding to Nile Red emission in pure water. Here, addition of acid leads to dissociation of the wormlike micelles, most likely due to dissociation of the imine surfactants to their water-soluble precursors, with the entire process taking place at a timescale of less than a minute. The demicellization was entirely reversible, as indicated by a blue shift of the NR emission maximum from 658 nm to 640 nm, when the pH of the acidic solution was changed back to its original alkaline state, upon addition of NaOH (aq.) In the absence of NR, the demicellization was accompanied by an immediate visual change of the solution from almost transparent and foaming to yellow and non-foaming (Figure 3b).

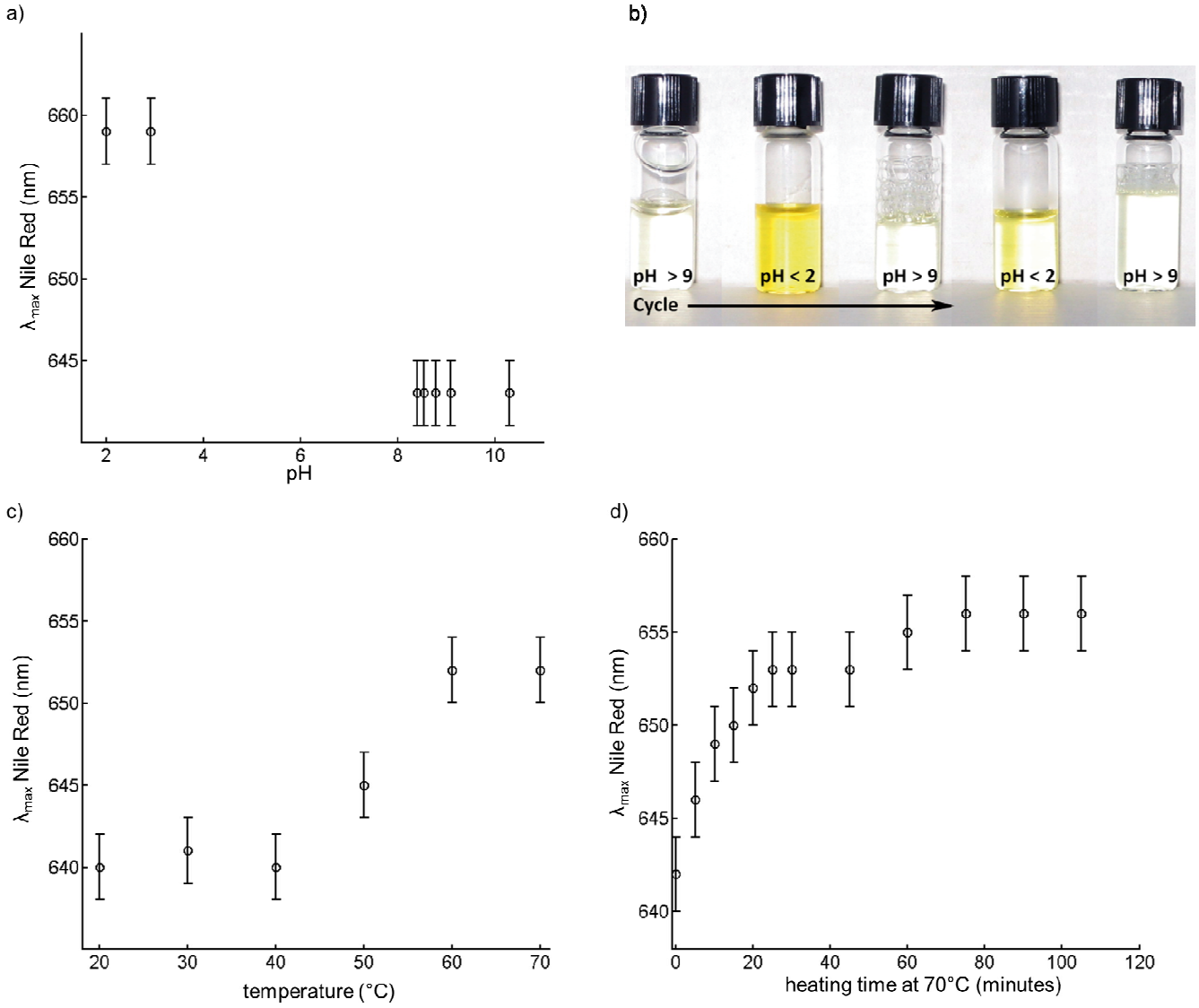

Figure 3. a) Nile Red maximum emission wavelength as a function of pH for **H₃●T₇**. b) pH switching of an **H₃●T₇** solution going from alkaline to acidic pH and back (samples without NR). c) Nile Red maximum emission wavelength as a function of temperature, starting at 20°C. The temperature of an 8 mM **H₃●T₇** solution (8 mM [**H₃**], 16 mM [**T₇**], pH 10.3), was increased to 70°C in steps of 10°C. d) An 8 mM **H₃●T₇** solution (8 mM [**H₃**], 16 mM [**T₇**], pH 10.3, 20°C) was directly heated to 70°C and Nile Red emission was studied over time.

As a second stimulus we used temperature to trigger demicellization, following the Nile Red emission as a function of temperature upon heating an **H₃●T₇** solution (8 mM [**H₃**], 16 mM [**T₇**]), solution equilibrated at pH 10.3). Each 15 minutes, the sample was heated up by 10°C, overall going from 20°C

to 70°C. We observed a redshift in Nile Red emission from 640 to 652 nm upon heating from 40 to 70°C, indicative of a significant destabilization of the $\mathbf{H_3 \bullet T_7}$ aggregates (Figure 3c). However, the applied heating times were too short to completely dissociate the aggregates. Therefore we heated a freshly prepared $\mathbf{H_3 \bullet T_7}$ solution ((8 mM [$\mathbf{H_3}$], 16 mM [$\mathbf{T_7}$]), solution equilibrated at pH 10.3) directly to 70°C and studied the Nile Red emission in time. These results showed that after 75 minutes heating a plateau region in Nile Red emission was observed at 657 nm, which is indicative for complete aggregate dissociation (Figure 3d). When cooling a 70°C surfactant solution back to 25°C, within minutes a blue shift to 640 nm was observed, which implies that heat-induced demicellization was entirely reversible upon cooling.

Conclusion

We have shown the spontaneous formation of dynamic covalent wormlike micelles from imine-based gemini surfactants, formed upon mixing aqueous solutions of two complementary non-surface active precursors. Our results indicate that the worm-like micelles are equilibrium structures from dynamic covalent surfactants, which are formed in situ by mixing of aqueous solutions of the precursors, without the need to synthesize the imine surfactant molecules separately. Similar results have been obtained before for closely related imine-based single and double tail dynamic covalent surfactants forming micelle and vesicles, respectively.[35,36] Thermodynamic modeling of the reaction and association equilibria shows that, although mixtures of surfactants are formed, it is primarily the double tailed surfactant that assembles into the wormlike micelles. The rheological properties of the wormlike micelles are near Newtonian, which we attribute to the short micellar lengths as observed by DLS and cryo-TEM. Resulting from the reversibility of the dynamic covalent imine bond, the wormlike micelles can be switched between an isotropic solution and the assembled state, triggered by pH and temperature, which is of particular interest for future drug delivery applications.

Acknowledgment: This work was supported by the Netherlands Organization for Scientific Research (NWO), STW/Nanoned (C.B.M.) and the European Commission (Marie Curie European Reintegration Grant (R.E.)). We are grateful to Krishna N. K. Kowlgi for his help with the DLS analysis.

Supporting Information Available: Details of synthesis and experimental techniques. This information is available free of charge via the Internet at http://pubs.acs.org/.

References

(1) Kirby, A.; Camilleri, J. P.; Engberts, J. B. F. N.; Feiters, M. C.; Nolte, R. J. M.; Söderman, O.; Bergsma, M.; Bell, P.C.; Fielden, M. L.; García Rodríguez, C. L.; Guédat, P.; Kremer, A.; McGregor, C.; Perrin, C.; Ronsin G.; van Eijk M. C. P. Gemini Surfactants: New Synthetic Vectors for Gene Transfection. *Angew. Chem. Int. Ed.* **2003**, *42*, 1448−1457.

(2) Dreiss, C. A. Wormlike Micelles: Where Do We Stand? Recent Developments, Linear Rheology and Scattering Techniques. *Soft Matter* **2007**, *3*, 956−970.

(3) Ezrahi, S.; Tuval, E.; Aserin, A. Properties, Main Applications and Perspectives of Worm Micelles. *Adv. Colloid. Interface. Sci.* **2006**, *128*, 77−102.

(4) Menger, F. M.; Keiper, J. S. Gemini Surfactants. *Angew. Chem. Int. Ed.* **2000**, *39*, 1906−1920.

(5) Aswal, V.; De, S.; Goyal. P. S.; Bhattacharya, S.; Heenan, R. K. Transition from Disc to Rod-like Shape of 16-3-16 Dimeric Micelles in Aqueous Solutions. *J. Chem. Soc. Faraday Trans.* **1998**, *94*, 2965−2967.

(6) Danino, D.; Talmon, Y.; Zana, R. Alkanediyl-alpha,omega-bis(dimethylalkylammonium bromide) Surfactants (Dimeric Surfactants). 5. Aggregation and Microstructure in Aqueous Solutions. *Langmuir* **1995**, 11, 1448−1456.

(7) Schmitt, V.; Schosseler, F.; Lequeux, F. Structure of Salt-free Wormlike Micelles - Signature by SANS at Rest and under Shear. *Europhys. Lett.* **1995**, *30*, 31−36.

(8) Pei, X.; Zhao, J.; Ye, Y.; Youa, Y.; Wei, X. Wormlike Micelles and Gels Reinforced by Hydrogen Bonding in Aqueous Cationic Gemini Surfactant Systems. *Soft Matter* **2011**, *7*, 2953−2960.

(9) Zana, R. Dimeric and Oligomeric Surfactants. Behavior at Interfaces and in Aqueous Solution: a Review. *Adv. Colloid. Interface. Sci.* **2002**, *97*, 205−253.

(10) Oda, R.; Huc, I.; Candau, S. J. Gemini Surfactants as New, Low Molecular Weight Gelators of Organic Solvents and Water. *Angew. Chem. Int. Ed.* **1998**, *37*, 2689−2691.

(11) Oda, R.; Huc, I.; Candau, S. J. Gemini Surfactants, the Effect of Hydrophobic Chain Length and Dissymmetry. *Chem. Commun.* **1997**, 2105−2106.

(12) Johnsson, M.; Engberts, J. B. F. N. Novel Sugar-based Gemini Surfactants: Aggregation Properties in Aqueous Solution. *J. Phys. Org. Chem.* **2004**, *17*, 934−944.

(13) Kumar, R.; Kalur, G. C.; Ziserman, L.; Danino, D.; Raghavan, S. R. Wormlike Micelles of a C22-Tailed Zwitterionic Betaine Surfactant: From Viscoelastic Solutions to Elastic Gels. *Langmuir* **2007**, *23*, 12849−12856.

(14) Almeida, J. A. S.; Marques, E. F.; Jurado, A. S.; Pais, A. A. C. C. The Effect of Cationic Gemini Surfactants upon Lipid Membranes. An Experimental and Molecular Dynamics Simulation Study. *Phys. Chem. Chem. Phys.* **2010**, *12*, 14462−14476.

(15) Scarzello, M.; Klijn, J. E.; Wagenaar, A.; Stuart, M. C. A.; Hulst, R.; Engberts, J. B. F. N. pH-Dependent Aggregation Properties of Mixtures of Sugar-based Gemini Surfactants with Phospholipids and Single-tailed Surfactants. *Langmuir* **2006**, *22*, 2558−2568.

(16) Fan, Y.R.; Li, Y.J.; Cao, M.W.; Wang, J.; Wang, Y.L. Thomas, R. K. Micellization of Dissymmetric Cationic Gemini Surfactants and their Interaction with Dimyristoylphosphatidylcholine Vesicles. *Langmuir* **2007**, *23*, 11458−11464.

(17) Klijn, J. E.; Stuart, M. C. A.; Scarzello, M.; Wagenaar, A.; Engberts, J. B. F. N. pH-Dependent Phase Behavior of Carbohydrate-based Gemini Surfactants. The Effects of Carbohydrate Stereochemistry, Head Group Hydrophilicity, and Nature of the Spacer. *J. Phys. Chem. B* **2007**, *111*, 5204−5211.

(18) Klijn, J. E.; Stuart, M. C. A.; Scarzello, M.; Wagenaar, A.; Engberts, J. B. F. N. pH-Dependent Phase Behavior of Carbohydrate-based Gemini Surfactants. Effect of the Length of the Hydrophobic Spacer. *J. Phys. Chem. B.* **2006**, *110*, 21694−21700.

(19) Lin, Y. Y.; Han, X.; Huang, J. B.; Fu, H. L.; Yu, C. L. A Facile Route to Design pH-Responsive Viscoelastic Wormlike Micelles: Smart Use of Hydrotropes. *J. Colloid. Interface. Sci.* **2009**, *330*, 449−455.

(20) Chu, Z.; Feng, Y. pH-Switchable Wormlike Micelles. *Chem. Commun.* **2010**, 9028−9030.

(21) Otto, S.; Furlan, R. L. E.; Sanders, J. K. M. Selection and Amplification of Hosts From Dynamic Combinatorial Libraries of Macrocyclic Disulfides. *Science* **2002**, *297*, 590−593.

(22) Huc, I.; Lehn, J. M. Virtual Combinatorial Libraries: Dynamic Generation of Molecular and Supramolecular Diversity by Self-Assembly. *Proc. Natl. Acad. Sci. USA* **1997**, *94*, 2106−2110.

(23) Lehn, J. M.; Eliseev, A. V. Dynamic Combinatorial Chemistry. *Science* **2001**, *291*, 2331−2332.

(24) Corbett, P. T.; Leclaire, J.; Vial, L.; West, K. R.; Wietor, J.; Sanders, J. K. M.; Otto, S. Dynamic Combinatorial Chemistry. *Chem. Rev.* **2006**, *106*, 3652−3711.

(25) Lehn, J. M. Chemistry - Dynamic Combinatorial Chemistry. *Science* **2002**, *295*, 2400−2403.

(26) Jackson, A. W.; Fulton, D. A. The Formation of Core Cross-linked Star Polymers Containing Cores Cross-linked by Dynamic Covalent Imine Bonds. *Chem. Commun.* **2010**, 6051−6053.

(27) Ono, T.; Fujii, S.; Nobori, T.; Lehn, J. M. Optodynamers: Expression of Color and Fluorescence at the Interface between Two Films of Different Dynamic Polymers. *Chem. Commun.* **2007**, 4360−4362.

(28) Moulin, E.; Cormosw, G.; Giuseppone, N. Dynamic Combinatorial Chemistry as a Tool for the Design of Functional Materials and Devices. *Chem. Soc. Rev.* **2012**, *41*, 1031−1049.

(29) Hunta, R. A. R.; Otto, S. Dynamic Combinatorial Libraries: New Opportunities in Systems Chemistry. *Chem. Commun.* **2011**, *47*, 847−858.

(30) Ghoussoub, A.; Lehn, J. M. Dynamic Sol-Gel Interconversion by Reversible Cation Binding and Release in G-Quartet-based Supramolecular Polymers. *Chem. Commun.* **2005**, 5763−5765.

(31) Sreenivasachary, N.; Lehn, J. M. Gelation-driven Component Selection in the Generation of Constitutional Dynamic Hydrogels based on Guanine-quartet Formation. *Proc. Natl. Acad. Sci. USA* **2005**, *102*, 5938−5943.

(32) Williams, R. J.; Smith, A. M.; Collins, R.; Hodson, N.; Das, A. K.; Ulijn, R. V. Enzyme-assisted Self-Assembly under Thermodynamic Control**.** *Nature Nanotechnol.* **2009**, *4*, 19−24.

(33) Folmer-Andersen, J. F.; Lehn, J. M.; Constitutional Adaptation of Dynamic Polymers: Hydrophobically Driven Sequence Selection in Dynamic Covalent Polyacylhydrazones. *Angew. Chem. Int. Ed.* **2009**, *48*, 7664−7667.

(34) Carnall, J. M. A.; Waudby, C. A.; Belenguer, A. M.; Stuart, M. C. A.; Peyralans, J. J. P.; Otto, S. Mechanosensitive Self-Replication Driven by Self-Organization. *Science* **2010**, *327*, 1502-1506.

(35) Minkenberg, C. B.; Florusse, L.; Eelkema, R.; Koper, G. J. M.; van Esch, J. H. Triggered Self-Assembly of Simple Dynamic Covalent Surfactants. *J. Am. Chem. Soc.* **2009**, *131*, 11274−11275.

(36) Minkenberg, C. B.; Li, F.; van Rijn, P.; Florusse, L.; Boekhoven, J.; Stuart, M. C. A.; Koper, G. J. M.; Eelkema, R.; van Esch, J. H. Responsive Vesicles from Dynamic Covalent Surfactants. *Angew. Chem. Int. Ed.* **2011**, *50*, 3421−3424.

(37) Nguyen, R.; Allouche, L.; Buhler, E.; Giuseppone, N. Dynamic Combinatorial Evolution within Self-Replicating Supramolecular Assemblies. *Angew. Chem. Int. Ed.* **2009**, *48*, 1093−1096.

(38) Wang, G. T.; Wang, C.; Wang, Z. Q.; Zhang, X. Bolaform Superamphiphile Based on a Dynamic Covalent Bond and its Self-Assembly in Water. *Langmuir* **2011**, *27*, 12375−12380.

(39) Wang, C.; Wang, Z.; Zhang, X. Amphiphilic Building Blocks for Self-Assembly: from Amphiphiles to Supra-amphiphiles. *Acc. Chem. Res.* **2012**, *45*, 608−618.

(40) Jouault, N.; Nguyen, R.; Rawiso, M.; Giuseppone, N.; Buhler, E. SANS, SAXS, and Light Scattering Investigations of pH-Responsive Dynamic Combinatorial Mesophases. *Soft Matter* **2011**, *7*, 4787−4800.

(41) Stephenson, R. M. Mutual Solubility of Water and Aliphatic Amines. *J. Chem. Eng. Data* **1993**, *38*, 625−629.

(42) Sackett, D. L.; Wolff, J. Nile Red as a Polarity-Sensitive Fluorescent-Probe of Hydrophobic Protein Surfaces. *Anal. Biochem.* **1987**, *167*, 228−234.

(43) Stuart, M. C. A.; van de Pas, J. C.; Engberts, J. B. F. N. The Use of Nile Red to Monitor the Aggregation Behavior in Ternary Surfactant-Water-Organic Solvent Systems. *J. Phys. Org. Chem.* **2005**, *18*, 929−934.

(44) Tlusty, T.; Safran, S. A.; Strey, R. Topology, Phase Instabilities, and Wetting of Microemulsion Networks. *Phys. Rev. Let.* **2000**, *84*, 1244−1247.

(45) Cates, M. E.; Candau, S. J. Statics and Dynamics of Worm-like Surfactant Micelles. *J. Phys.: Condens. Matter* **1990**, *2*, 6869−6892.

(46) Kern, F.; Lequeux, F.; Zana, R.; Candau, S. J. Dynamical Properties of Salt-free Viscoelastic Micellar Solutions. *Langmuir* **1994**, *10*, 1714−1723.

(47) In, M.; Bec, V.; Aguerre-Chariol, O.; Zana, R. Quaternary Ammonium Bromide Surfactant Oligomers in Aqueous Solution: Self-Association and Microstructure. *Langmuir* **2000**, *16*, 141−148.

(48) Han, L.; Chen, H.; Luo, P. Viscosity Behavior of Cationic Gemini Surfactants with Long Alkyl Chains. *Surface Sci.* **2004**, *564*, 141−148.

Table of Contents only

